Electronic Supplementary Material (ESI) for Environmental Science: Nano.
This journal is © The Royal Society of Chemistry 2019

Supporting Information for:

How Nanoscale Surface Heterogeneity Impacts Transport of Nano- to Micro-Particles on Surfaces under Unfavorable Attachment Conditions

Cesar A. Ron[1], Kurt VanNess[1], Anna Rasmuson[1], William P. Johnson[1]*.

[1]Department of Geology & Geophysics, University of Utah, Salt Lake City, UT 84112, USA

Table SI-1. ζ-potential values used in simulations for CML=carboxylate modified polystyrene latex, CMS= carboxylate modified silica, UMS=unmodified silica. Values were determined from EPM measurements via the Smoluchowski equation[1]. Note that measurements for colloids > 3 μm have inherent uncertainty using this method.

Material	Colloid Diameter (μm)	NaCl (mM)	pH	ζ-potential (mV)
CML	0.1	6.0	6.7	-45.3
CML	0.3	6.0	6.7	-18.3
CML	1.1	6.0	6.7	-65.4
CML	2.0	6.0	6.7	-29.9
CML	4.4	6.0	6.7	-65.0
CML	6.8	6.0	6.7	-10.2
CML	0.1	20.0	6.7	-35.9
CML	0.3	20.0	6.7	-10.5
CML	1.1	20.0	6.7	-50.1
CML	2.0	20.0	6.7	-8.2
CML	4.4	20.0	6.7	-42.8
CML	6.8	20.0	6.7	-4.5
CML	0.1	6.0	8.0	-61.4
CML	0.3	6.0	8.0	-74.9
CML	1.1	6.0	8.0	-91.0
CML	2.0	6.0	8.0	-80.5
CML	4.4	6.0	8.0	-52.0
CML	6.8	6.0	8.0	-6.9
CML	0.1	20.0	8.0	-42.0
CML	0.3	20.0	8.0	-26.5
CML	1.1	20.0	8.0	-62.2
CML	2.0	20.0	8.0	-63.9
CML	4.4	20.0	8.0	-63.1
CML	6.8	20.0	8.0	-11.8
CML	0.1	50.0	2.0	-13.8
CML	0.3	50.0	2.0	-2.3
CML	1.1	50.0	2.0	-5.1
CML	2.0	50.0	2.0	-5.4
CML	4.4	50.0	2.0	-11.7
CML	6.8	50.0	2.0	1.9
CMS	1.0	6.0	6.7	-66.7
CMS	3.0	6.0	6.7	-15.4
UMS	3.0	6.0	6.7	-27.6
CMS	1.0	50.0	2.0	5.1
CMS	3.0	50.0	2.0	37.4
UMS	3.0	50.0	2.0	-1.7

Table SI-2. ζ-potential values used in simulations for soda-lime glass collector surface (silica). ζ-potential were from representative values reported in the literature.

Material	NaCl (mM)	pH	ζ-potential (mV)
Glass[2]	6.0	6.7	-70.0
Glass[2]	20.0	6.7	-53.5
Glass[2]	6.0	8.0	-80.0
Glass[2]	20.0	8.0	-70.0
Glass[3]	50.0	2.0	-10.0

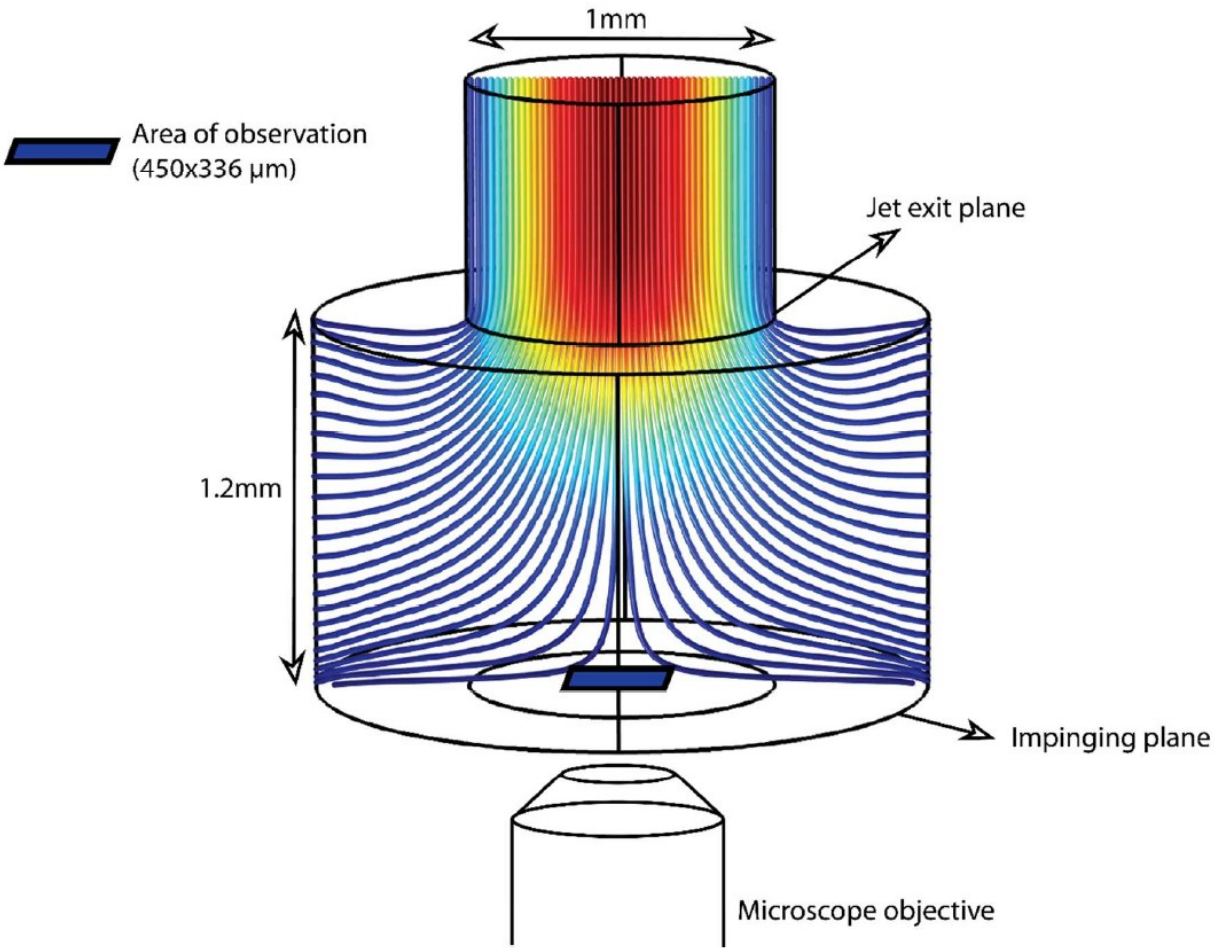

Figure SI-1. Schematic of the impinging jet flow chamber. Fluid flow field is represented by color coded low lines (red high velocity, blue low velocity). The jet is 0.5 mm in radius and the impinging plane is located 1.25 mm below the jet exit. Images of attached colloids are acquired via an inverted microscope across an area of observation of 450x336 μm on the impinging plane aligned with the center of the jet.[4–6]

Table SI-3. RMS roughness values used in simulations regarding attachment of CML onto silica surfaces. Roughness values were determined as desribed in Rasmuson et al.[7]

CML diameter (μm)	RMS roughness (nm)
0.1	4.7
0.25	6.4
1.1	10.3
2.0	13.0
4.4	17.0
6.8	19.8

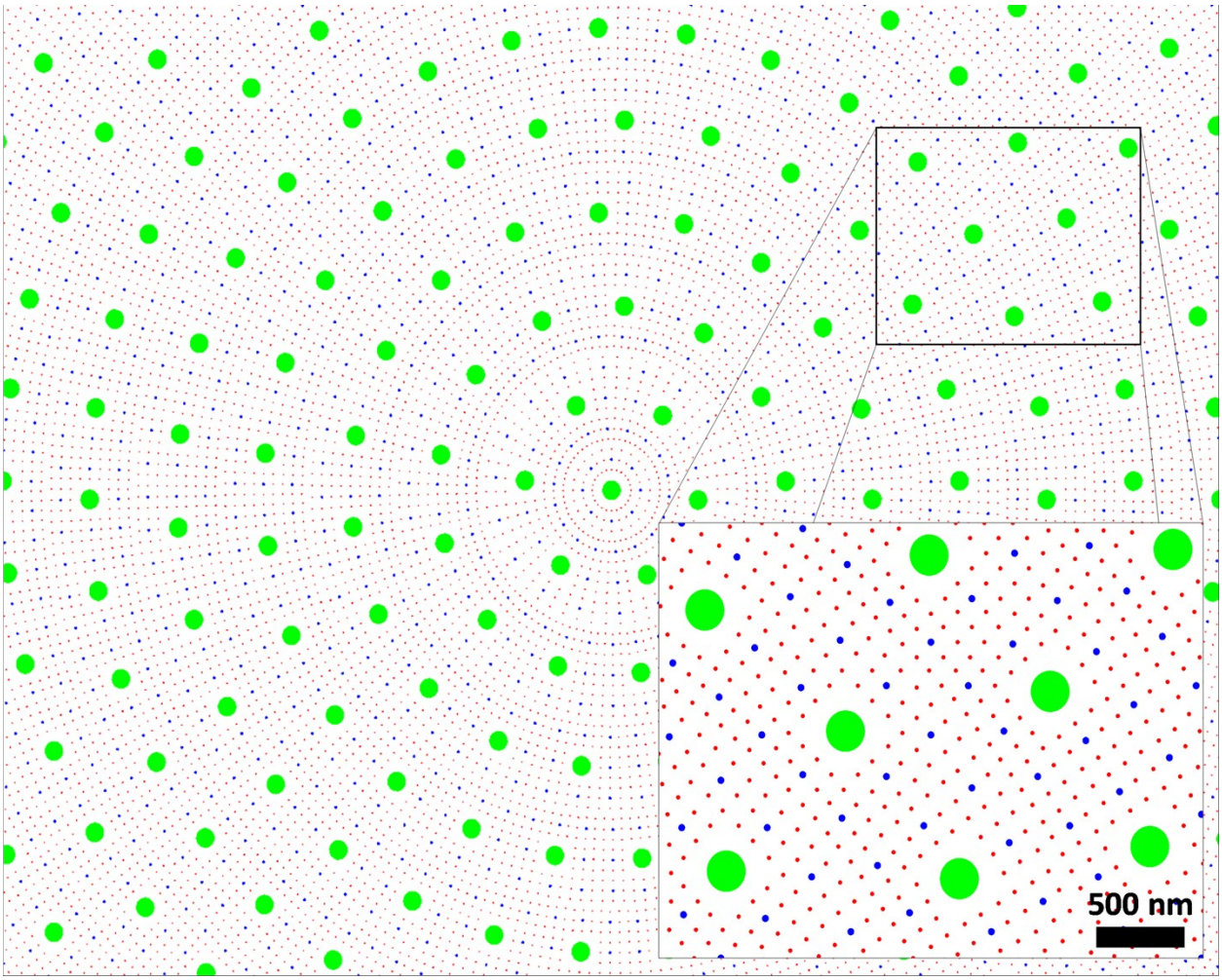

Figure SI-2. Representation of DRNH using power law-distributed heterodomains of three different sizes (green: 220 nm, blue: 40 nm, and red: 25 nm) increasing frequency ratios (1:8:64) superimposed onto the same surface. In simulations, the pattern was expanded to cover the entire surface at a defined spatial density (SD).

Table SI-4. Deposition rate constants (k_f), collector efficiencies (η), and collision efficiencies (α) from published literature meeting criteria provided in main text.

							***kf* (1/s)**		***η***		
Colloid	**Colloid diameter (μm)**	**Surface**	**Grain diameter (μm)**	**Vpore (m/day)**	**pH**	**IS (mM)**	**Favorable**	**Unfavorable**	**Favorable**	**Unfavorable**	**α**
Cryptosporidium parvum Oocysts[8]	4.100	Silicate sand	375.0	18.506	8.0	1.0	2.46E-03	3.36E-03	5.03E-03	6.86E-03	1.363
Copolymer-modified Latex Microspheres[8]	4.300	Silicate sand	375.0	18.506	8.0	1.0	2.48E-03	3.31E-03	5.07E-03	6.75E-03	1.331
Anatase[9]	0.198	Silicate sand	358.5	101.647	7.0	10.0	1.67E-02	1.52E-03	5.11E-03	4.66E-04	0.091
CML[3]	0.110	Glass beads	508.5	4.000	6.7	20.0	2.78E-03	2.00E-04	3.23E-02	2.36E-03	0.073
CML[3]	0.200	Glass beads	508.5	4.000	6.7	20.0	2.22E-03	7.22E-05	2.59E-02	8.53E-04	0.033
CML[3]	0.500	Glass beads	508.5	4.000	6.7	20.0	1.81E-03	1.75E-05	2.11E-02	2.07E-04	0.010
CML[3]	1.000	Glass beads	508.5	4.000	6.7	20.0	1.11E-03	6.94E-05	1.30E-02	8.20E-04	0.063
CML[3]	2.000	Glass beads	508.5	4.000	6.7	20.0	1.14E-03	2.56E-04	1.34E-02	3.01E-03	0.226
MS2[10]	0.025	Ohio river sand	245.0	38.750	7.0	6.8	1.77E-01	2.91E-04	9.05E-02	1.56E-04	0.002
PRD1[10]	0.065	Ohio river sand	245.0	38.750	7.0	6.8	8.07E-02	9.87E-05	4.23E-02	5.29E-05	0.001
OY107[10]	0.690	Ohio river sand	245.0	38.750	7.0	6.8	1.26E-02	2.70E-05	6.74E-03	1.45E-05	0.002
DA001[10]	0.850	Ohio river sand	245.0	38.750	7.0	6.8	1.10E-02	5.72E-05	5.87E-03	3.06E-05	0.005
E. Coli[10]	1.000	Ohio river sand	245.0	38.750	7.0	6.8	1.00E-02	5.73E-05	5.34E-03	3.07E-05	0.006
Cryptosporidium parvum Oocysts [10]	5.500	Ohio river sand	245.0	38.750	7.0	6.8	2.17E-02	1.83E-02	1.16E-02	9.75E-03	0.842
Cryptosporidium parvum Oocysts[11]	4.000	Glass beads	328.0	19.382	8.0	10.0	5.80E-03	1.70E-03	8.94E-03	2.63E-03	0.294
Carboxylate-modified Latex Microspheres[11]	3.000	Glass beads	328.0	19.382	8.0	10.0	4.17E-03	1.29E-04	6.43E-03	2.00E-04	0.031

Table SI-4 (Continued). Deposition rate constants (k_f), collector efficiencies (η), and collision efficiencies (α)

Cerium Oxide[12]	0.063	Silicate sand	717.0	167.169	6.0	1.0	8.72E-03	3.23E-03	3.26E-03	1.21E-03	0.370
Silica[13]	0.052	Silicate sand	220.0	3.710	10.0	1.0	5.97E-02	8.89E-06	2.66E-01	4.60E-05	0.000
Silica[13]	0.008	Silicate sand	220.0	3.710	10.0	1.0	8.26E-01	4.17E-05	9.86E-01	2.16E-04	0.000
Zinc Oxide[14]	0.300	Quartz sand	510.0	8.023	8.0	5.0	3.29E-03	4.72E-04	2.06E-02	2.98E-03	0.145
Rutile[15]	0.149	Quartz sand	275.0	11.909	6.0	1.0	2.06E-02	6.37E-04	4.25E-02	1.34E-03	0.032
Zero valent Iron[16]	0.065	Quartz sand	725.0	73.339	8.0	-	1.09E-02	5.37E-03	1.03E-02	5.08E-03	0.494
DA001[17]	1.100	Glass beads	508.5	4.002	6-9	4.0	1.11E-03	5.56E-05	1.30E-02	6.56E-04	0.050
Escherichia Coli D21g[18]	1.700	Quartz sand	205.0	42.195	5.7	3.2	1.11E-03	2.40E-04	1.30E-02	1.18E-04	0.009
Escherichia Coli D21g[19]	0.960	Quartz sand	275.0	31.930	5.7	10.0	1.70E-02	6.00E-04	1.55E-02	5.51E-04	0.036
Escherichia Coli XL1-Blue[19]	1.100	Quartz sand	275.0	31.930	5.7	10.0	1.70E-02	4.80E-04	1.55E-02	4.41E-04	0.028
Carboxylate-modified latex microspheres(This study)	0.110	Soda-lime glass	Impinging jet	2.000	6.7	6.0	-	-	0.000114	4.70309E-05	0.413
Carboxylate-modified latex microspheres(This study)	0.250	Soda-lime glass	Impinging jet	2.000	6.7	6.0	-	-	3.16E-05	6.27953E-06	0.199
Carboxylate-modified latex microspheres(This study)	1.100	Soda-lime glass	Impinging jet	2.000	6.7	6.0	-	-	1.94E-05	1.85494E-06	0.096
Carboxylate-modified latex microspheres(This study)	2.000	Soda-lime glass	Impinging jet	2.000	6.7	6.0	-	-	1.06E-05	1.51048E-06	0.143
Carboxylate-modified latex microspheres(This study)	4.400	Soda-lime glass	Impinging jet	2.000	6.7	6.0	-	-	4.15E-05	3.03814E-05	0.732
Carboxylate-modified latex microspheres(This study)	6.800	Soda-lime glass	Impinging jet	2.000	6.7	6.0	-	-	0.000178	0.0000919	0.518
Carboxylate-modified latex microspheres(This study)	0.110	Soda-lime glass	Impinging jet	2.000	6.7	20.0	-	-	0.000114	5.38031E-05	0.473
Carboxylate-modified latex microspheres(This study)	0.250	Soda-lime glass	Impinging jet	2.000	6.7	20.0	-	-	3.16E-05	1.6654E-05	0.528
Carboxylate-modified latex microspheres(This study)	1.100	Soda-lime glass	Impinging jet	2.000	6.7	20.0	-	-	1.94E-05	4.36965E-06	0.225

Table SI-4 (Continued). Deposition rate constants (k_f), collector efficiencies (η), and collision efficiencies (α)

Carboxylate-modified latex microspheres(This study)	2.000	Soda-lime glass	Impinging jet	2.000	6.7	20.0	-	-	1.06E-05	5.2718E-06	0.498
Carboxylate-modified latex microspheres(This study)	4.400	Soda-lime glass	Impinging jet	2.000	6.7	20.0	-	-	4.15E-05	4.74588E-05	1.144
Carboxylate-modified latex microspheres(This study)	6.800	Soda-lime glass	Impinging jet	2.000	6.7	20.0	-	-	0.000178	0.000122502	0.690
Carboxylate-modified latex microspheres(This study)	0.110	Soda-lime glass	Impinging jet	2.000	8.0	6.0	-	-	0.000114	2.1338E-05	0.188
Carboxylate-modified latex microspheres(This study)	0.250	Soda-lime glass	Impinging jet	2.000	8.0	6.0	-	-	3.16E-05	4.62587E-07	0.015
Carboxylate-modified latex microspheres(This study)	1.100	Soda-lime glass	Impinging jet	2.000	8.0	6.0	-	-	1.94E-05	7.55524E-08	0.004
Carboxylate-modified latex microspheres(This study)	2.000	Soda-lime glass	Impinging jet	2.000	8.0	6.0	-	-	1.06E-05	1.60113E-07	0.015
Carboxylate-modified latex microspheres(This study)	4.400	Soda-lime glass	Impinging jet	2.000	8.0	6.0	-	-	4.15E-05	3.03814E-05	0.732
Carboxylate-modified latex microspheres(This study)	6.800	Soda-lime glass	Impinging jet	2.000	8.0	6.0	-	-	0.000178	0.000108403	0.611
Carboxylate-modified latex microspheres(This study)	0.110	Soda-lime glass	Impinging jet	2.000	8.0	20.0	-	-	0.000114	1.47937E-05	0.130
Carboxylate-modified latex microspheres(This study)	0.250	Soda-lime glass	Impinging jet	2.000	8.0	20.0	-	-	3.16E-05	5.19027E-06	0.164
Carboxylate-modified latex microspheres(This study)	1.100	Soda-lime glass	Impinging jet	2.000	8.0	20.0	-	-	1.94E-05	3.65429E-07	0.019
Carboxylate-modified latex microspheres(This study)	2.000	Soda-lime glass	Impinging jet	2.000	8.0	20.0	-	-	1.06E-05	4.96712E-07	0.047
Carboxylate-modified latex microspheres(This study)	4.400	Soda-lime glass	Impinging jet	2.000	8.0	20.0	-	-	4.15E-05	1.85407E-05	0.447
Carboxylate-modified latex microspheres(This study)	6.800	Soda-lime glass	Impinging jet	2.000	8.0	20.0	-	-	0.000178	0.000201867	1.137
Carboxylate-modified silica microspheres(This study)	1.000	Soda-lime glass	Impinging jet	2.000	6.7	6.0	-	-	9.33E-05	2.21681E-06	0.024
Carboxylate-modified silica microspheres(This study)	3.000	Soda-lime glass	Impinging jet	2.000	6.7	6.0	-	-	0.000366	0.000387712	1.060

References Cited

1 H. Ohshima, Electrophoresis of soft particles: Analytic approximations, *Electrophoresis*, 2006, **27**, 526–533.

2 B. J. Kirby and E. F. Hasselbrink, Zeta potential of microfluidic substrates: 1. Theory, experimental techniques, and effects on separations, *Electrophoresis*, 2004, **25**, 187–202.

3 M. Tong and W. P. Johnson, Excess colloid retention in porous media as a function of colloid size, fluid velocity, and grain angularity, *Environ. Sci. Technol.*, 2006, **40**, 7725–7731.

4 E. Pazmino, J. Trauscht, B. Dame and W. P. Johnson, Power Law Size-Distributed Heterogeneity Explains Colloid Retention on Soda Lime Glass in the Presence of Energy Barriers, *Langmuir*, 2014, **30**, 5412–5421.

5 J. Trauscht, E. Pazmino and W. P. Johnson, Prediction of Nanoparticle and Colloid Attachment on Unfavorable Mineral Surfaces Using Representative Discrete Heterogeneity, *Langmuir*, 2015, **31**, 9366–9378.

6 M. Hilpert, A. Rasmuson and W. P. Johnson, A binomial modeling approach for upscaling colloid transport under unfavorable conditions: Emergent prediction of extended tailing, *Water Resour. Res.*, 2017, **53**, 5626–5644.

7 A. Rasmuson, K. VanNess, C. Ron and W. P. Johnson, Hydrodynamic versus Surface Interaction Impacts of Roughness in Closing the Gap between Favorable and Unfavorable Colloid Transport Conditions, *Environ. Sci. Technol.*, 2019, **53**, 2450–2459.

8 L. Liu, Y. Wang, R. Narain and Y. Liu, Functionalized polystyrene microspheres as Cryptosporidium surrogates, *Colloids Surfaces B Biointerfaces*, 2019, **175**, 680–687.

9 H. F. Lecoanet, J. Y. Bottero and M. R. Wiesner, Laboratory assessment of the mobility of nanomaterials in porous media, *Environ. Sci. Technol.*, 2004, **38**, 5164–5169.

10 V. Gupta, W. P. Johnson, P. Shafieian, H. Ryu, A. Alum, M. Abbaszadegan, S. A. Hubbs and T. Rauch-Williams, Riverbank filtration: Comparison of pilot scale transport with theory, *Environ. Sci. Technol.*, 2009, **43**, 669–676.

11 N. Tufenkji and M. Elimelech, Spatial distributions of Cryptosporidium oocysts in porous media: Evidence for dual mode deposition, *Environ. Sci. Technol.*, 2005, **39**, 3620–3629.

12 Z. Li, E. Sahle-Demessie, A. A. Hassan and G. A. Sorial, Transport and deposition of CeO2 nanoparticles in water-saturated porous media, *Water Res.*, 2011, **45**, 4409–4418.

13 C. Wang, A. D. Bobba, R. Attinti, C. Shen, V. Lazouskaya, L. P. Wang and Y. Jin, Retention and transport of silica nanoparticles in saturated porous media: Effect of concentration and particle size, *Environ. Sci. Technol.*, 2012, **46**, 7151–7158.

14 X. Jiang, M. Tong, R. Lu and H. Kim, Transport and deposition of ZnO nanoparticles in saturated porous media, *Colloids Surfaces A Physicochem. Eng. Asp.*, 2012, **401**, 29–37.

15 G. Chen, X. Liu and C. Su, Transport and retention of TiO2 rutile nanoparticles in saturated porous media under low-ionic-strength conditions: Measurements and mechanisms, *Langmuir*, 2011, **27**, 5393–5402.

16 P. Jiemvarangkul, W. X. Zhang and H. L. Lien, Enhanced transport of polyelectrolyte stabilized nanoscale zero-valent iron (nZVI) in porous media, *Chem. Eng. J.*, 2011, **170**, 482–491.

17 M. Tong, X. Li, C. N. Brow and W. P. Johnson, Detachment-influenced transport of an adhesion-deficient bacterial strain within water-reactive porous media, *Environ. Sci. Technol.*, 2005, **39**, 2500–2508.

18 J. A. Redman, S. L. Walker and M. Elimelech, Bacterial Adhesion and Transport in Porous Media: Role of the Secondary Energy Minimum, *Environ. Sci. Technol.*, 2004, **38**, 1777–1785.

19 H. N. Kim and S. L. Walker, Escherichia coli transport in porous media: Influence of cell strain, solution chemistry, and temperature, *Colloids Surfaces B Biointerfaces*, 2009, **71**, 160–167.